ELSEVIER

EMIL WOLF

EDITOR

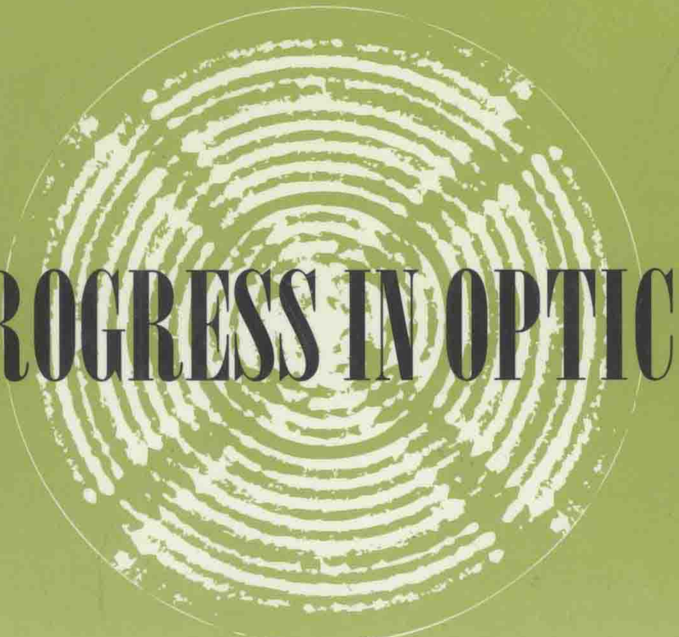

PROGRESS IN OPTICS

VOLUME 57

CONTRIBUTORS

V. Backman, B. Bhaduri, I. R. Çapoğlu, Z. Chen, L. Hua, D. Kroisova, M. Mir, G. Popescu, J. Pu, J. D. Rogers, A. Taflove, R. Wang, T. Wang, D. Zhao, R. Zhu

VOLUME FIFTY SEVEN

PROGRESS IN OPTICS

Edited by

E. WOLF

University of Rochester, N.Y., U.S.A.

Contributors

V. Backman, B. Bhaduri, İ. R. Çapoğlu, Z. Chen, L. Hua, D. Kroisova, M. Mir, G. Popescu, J. Pu, J. D. Rogers, A. Taflove, R. Wang, T. Wang, D. Zhao, R. Zhu

Amsterdam • Boston • Heidelberg • London • New York • Oxford
ELSEVIER Paris • San Diego • San Francisco • Singapore • Sydney • Tokyo

Elsevier
The Boulevard, Langford Lane, Kidlington, Oxford OX5 1GB, UK
Radarweg 29, PO Box 211, 1000 AE Amsterdam, The Netherlands

First edition 2012

Library of Congress Cataloging-in-Publication Data
A catalog record for this book is available from the Library of Congress

British Library Cataloguing-in-Publication Data
A catalogue record for this book is available from the British Library

ISBN: 978-0-44-459422-8
ISSN: 0079-6638

Printed and bounded in Great Britain
12 13 10 9 8 7 6 5 4 3 2 1

CONTRIBUTORS

Vadim Backman
Biomedical Engineering Department, Northwestern University, Evanston, IL, USA

Basanta Bhaduri
Quantitative Light Imaging Laboratory, Department of Electrical and Computer Engineering, Beckman Institute for Advanced Science and Technology, University of Illinois at Urbana-Champaign, Urbana, IL, USA

İlker R. Çapoğlu
Biomedical Engineering Department, Northwestern University, Evanston, IL, USA

Ziyang Chen
College of Information Science and Engineering, Huaqiao University, Xiamen, Fujian, China

Limin Hua
College of Information Science and Engineering, Huaqiao University, Xiamen, Fujian, China

Dora Kroisova
Technical University of Liberec, Department of Material Science, Studentska 2, Liberec, Czech Republic

Mustafa Mir
Quantitative Light Imaging Laboratory, Department of Electrical and Computer Engineering, Beckman Institute for Advanced Science and Technology, University of Illinois at Urbana-Champaign, Urbana, IL, USA

Gabriel Popescu
Quantitative Light Imaging Laboratory, Department of Electrical and Computer Engineering, Beckman Institute for Advanced Science and Technology, University of Illinois at Urbana-Champaign, Urbana, IL, USA

Jixiong Pu
College of Information Science and Engineering, Huaqiao University, Xiamen, Fujian, China

Jeremy D. Rogers
Biomedical Engineering Department, Northwestern University, Evanston, IL, USA

Allen Taflove
Electrical Engineering and Computer Science Department, Northwestern University, Evanston, IL, USA

Ru Wang
Quantitative Light Imaging Laboratory, Department of Electrical and Computer Engineering, Beckman Institute for Advanced Science and Technology, University of Illinois at Urbana-Champaign, Urbana, IL, USA

Tao Wang
Department of Physics, Zhejiang University, Hangzhou, China

Daomu Zhao
Department of Physics, Zhejiang University, Hangzhou, China

Ruoyu Zhu
Quantitative Light Imaging Laboratory, Department of Electrical and Computer Engineering, Beckman Institute for Advanced Science and Technology, University of Illinois at Urbana-Champaign, Urbana, IL, USA

PREFACE

This 57th volume of *Progress in Optics* presents reviews of five subjects which have become of considerable interest in recent years; namely, image synthesis from three-dimensional solutions of Maxwell's equations at the nanometer scale, direct and inverse problems in the theory of light scattering, tight focusing of light beams, nanostructures in natural materials, and quantitative phase imaging.

Emil Wolf
Department of Physics and Astronomy
and The Institute of Optics
University of Rochester
Rochester, New York, USA

June 2012

CONTENTS

CHAPTER ONE

The Microscope in a Computer: Image Synthesis from Three-Dimensional Full-Vector Solutions of Maxwell's Equations at the Nanometer Scale

İlker R. Çapoğlu[a], Jeremy D. Rogers[a], Allen Taflove[b] and Vadim Backman[a]
[a]Biomedical Engineering Department, Northwestern University, Evanston, IL, USA
[b]Electrical Engineering and Computer Science Department, Northwestern University, Evanston, IL, USA

Contents

Progress in Optics, Volume 57
ISSN 0079-6638, http://dx.doi.org/10.1016/B978-0-44-459422-8.00001-1

1. INTRODUCTION

Optical imaging systems have traditionally been analyzed using well-established approximations such as ray-based geometrical optics (Born & Wolf, 1999) and scalar Fourier theory (Goodman, 1996). However, there has recently been increased interest in applying the rigorous framework of Maxwell's-equations-based electromagnetic theory and numerical modeling to the analysis of optical imaging systems. The availability of more powerful computer hardware and more efficient computational algorithms has obviously contributed to this interest. Although the basic principles of light scattering encoded in Maxwell's equations had been around for decades, the widespread application of these principles to the complete modeling of an optical imaging system had to wait until the 1990s, at which time the personal computers were getting powerful enough to process megabytes of data in their memory. This allowed the modeling of objects that are comparable in size to the wavelength of the illuminating light (400–800 nm). With the arrival of these computational capabilities, the possibility of bypassing most of the traditional simplifying approximations and numerically calculating the optical image of an arbitrary object was at hand; and the demand for this accuracy was already present. Some engineering applications require the control of all the aspects of the optical imaging system down to sub-wavelength precision. Examples of such applications can be found in many subfields of physics and engineering. Historically, the earliest work on the numerical simulation of optical imaging was for modeling integrated-circuit production via photolithography (Cole, Barouch, Conrad, & Yeung, 2001; Neureuther, 2008), integrated-circuit inspection (Neureuther, 1992), and mark alignment (Nikolaev & Erdmann, 2003). More recently, there has been increasing interest in modeling optical microscopy modalities (Capoglu et al., 2011; Hollmann, Dunn, & DiMarzio, 2004; Sierra, DiMarzio, & Brooks, 2008; Simon & DiMarzio, 2007; Tanev, Pond, Paddon, & Tuchin, 2008; Tanev, Sun, Pond, Tuchin, & Zharov, 2009). If realized to its full potential, this technique could have immediate benefit on the optical detection of early stage nanoscale alterations in precancerous cells (Subramanian et al., 2008, 2009). This review/tutorial paper is primarily aimed as a reference for the numerical algorithms and techniques necessary for implementing a purely virtual imaging system, which we will refer to as a "microscope in a computer." Since the basic principles are also applicable to any other optical imaging system, this paper could also be consulted for modeling photolithography and metrology systems.

Although Maxwell's-equations-based electromagnetic principles have been successfully applied to the characterization of optical systems, the literature on the subject is fragmented across several independent lines of research, resulting in considerable overlap and inefficiency. This is a consequence of the fact that different forms of optical imaging systems are employed in many independent branches of engineering, sometimes based on similar principles but for diverse purposes. This fragmented literature has not yet been compiled and categorically documented for the benefit of the general engineering community. In this paper, we present a coherent and self-contained account of the numerical electromagnetic simulation of optical imaging systems, and review the body of work amassed in this rapidly growing field. We place special emphasis on numerical modeling issues such as discretization, sampling, and signal processing. Although the majority of the paper is tailored for optics, most of the concepts and formulas given in Section 2 and Sections 3.1–3.3 are applicable to a broader range of electromagnetics problems involving antennas, antenna arrays, metamaterials, RF, and microwave circuits and radars. The refocusing concept in Section 3.4, however, is a defining characteristic of an optical imaging system, with few exceptions such as focused antenna arrays in RF electromagnetics (Hansen, 1985).

The remainder of the paper is organized as follows. In Section 2, the basic principles of electromagnetics and optical coherence are reviewed. In Section 3, the optical imaging system is divided into fundamental components, and the numerical simulation of each component is described in detail. In Section 4, an optical imaging simulation system based on the finite-difference time-domain method is introduced, and several microscopy simulation examples are presented. A summary of our review and some concluding remarks are given in Section 5.

2. BASIC PRINCIPLES OF ELECTROMAGNETICS AND OPTICAL COHERENCE

An integral part of the numerical electromagnetic analysis of optical imaging systems is based on a set of vectorial relationships called *Maxwell's equations* that explain the propagation of light and its behavior in material media. These equations describe the nature and interrelationship of two vectorial quantities, the *electric* and *magnetic* field vectors $\boldsymbol{\mathcal{E}}(\boldsymbol{r}, t)$ and $\boldsymbol{\mathcal{H}}(\boldsymbol{r}, t)$, in free space and matter. The interaction of these vectors with matter is specified by two scalar material properties, the relative permittivity $\epsilon_r(\boldsymbol{r})$ and permeability $\mu_r(\boldsymbol{r})$. In crude terms, these two material properties quantify the response of matter to the electric and magnetic fields, respectively. In free space, these parameters are both equal to unity ($\epsilon_r = \mu_r = 1$). In differential form, Maxwell's equations are written as

$$\nabla \times \boldsymbol{\mathcal{E}} = -\mu_r \mu_0 \frac{d\boldsymbol{\mathcal{H}}}{dt}, \tag{1}$$

$$\nabla \times \boldsymbol{\mathcal{H}} = \boldsymbol{\mathcal{J}} + \epsilon_r \epsilon_0 \frac{d\boldsymbol{\mathcal{E}}}{dt}, \tag{2}$$

$$\nabla \cdot \boldsymbol{\mathcal{E}} = \rho, \tag{3}$$

$$\nabla \cdot \boldsymbol{\mathcal{H}} = 0, \tag{4}$$

where the symbol "$\nabla\times$" denotes the curl operator, which locally quantifies the amount and orientation of the "vorticity" in the vector field, and "$\nabla\cdot$" denotes the "div" operator, which quantifies the local magnitude of the "source" or "sink" associated with the vector field. Both definitions are in analogy to a velocity field in a fluid-dynamics context. In these equations, the electric current density $\boldsymbol{\mathcal{J}}(\boldsymbol{r}, t)$ acts as the excitation for the electromagnetic field. If the response of a system at a particular frequency of operation ω is of interest, Maxwell's equations simplify to their time-harmonic versions in which the time dependence is factored out in the form $\exp(j\omega t)$:

$$\nabla \times \boldsymbol{E} = -j\omega\mu_r\mu_0 \boldsymbol{H}, \tag{5}$$

$$\nabla \times \boldsymbol{H} = \boldsymbol{J} + j\omega\epsilon_r\epsilon_0 \boldsymbol{E}, \tag{6}$$

$$\nabla \cdot \boldsymbol{E} = \rho, \tag{7}$$

$$\nabla \cdot \boldsymbol{H} = 0. \tag{8}$$

Here and in what follows, calligraphic fonts $\mathcal{A}$, $\mathcal{B}$ will be used to denote general time dependence, while Roman fonts A, B will be used to denote time-harmonic quantities for which the time dependence $\exp(j\omega t)$ is implicit. In the engineering literature, it is customary to refer to Equations (1)–(4) as being in the *time domain*, and the time-harmonic versions (5)–(8) as being in the *frequency domain.*

In optics, the parameter $n = (\epsilon_r\mu_r)^{1/2}$ is called the *refractive index* of the medium. It relates the light velocity v in the medium to the velocity c in the vacuum as $v = c/n$. In electromagnetics, the expression $W_E = \epsilon_r\epsilon_0|\boldsymbol{E}(\boldsymbol{r})|^2/2$ is the average electrical energy density at a point in space (in SI units). In the geometrical-optics (small-wavelength) approximation, the radiated power per unit area in the local direction of propagation is equal to $I = 2(c/n)W_E$ (Born & Wolf, 1999). Assuming non-magnetic media ($\mu_r = 1$), this becomes

$$I = n|\boldsymbol{E}(\boldsymbol{r})|^2/\eta_0, \quad (9)$$

in which $\eta_0 = (\mu_0/\epsilon_0)^{1/2}$ is the *wave impedance* of free space. Although alternative terminologies do exist, we will use the term *light intensity* or simply *intensity* for the radiated power per unit area. The light intensity is a direct measure of the signal collected by recording media that convert light energy to other forms of energy. Examples of these recording media include photoresists, CCD cameras, and the retina. We will assume non-magnetic media throughout the paper and define the light intensity as in (9).

In most practical situations, the excitation in the optical system (whether it be a filament or a laser source) has a certain random character. This creates randomness in the resulting optical electromagnetic field in both space and time. If this is the case, the electromagnetic field may only be representable as a *random field* that possesses certain statistical properties. Fortunately, we are almost always concerned with time averages of optical parameters such as intensity or polarization, because these are the only parameters that most optical instruments can measure. If an adequate statistical model is constructed for the random electromagnetic field, the average quantities measured at the output of the system can be inferred mathematically. The categorization and rigorous mathematical description of these matters is the subject of *optical coherence* (Born & Wolf, 1999; Goodman, 2000). Although optical illumination systems almost always have a random character, the numerical electromagnetic simulation methods considered in this paper operate on deterministic field values that are known precisely in space and time. Numerical solutions of differential equations that operate directly on statistically averaged values [such as the radiative transfer equation (Ishimaru, 1999)] are outside the scope of this paper; see (Arridge & Hebden, 1997) for a review of these methods. The question arises, therefore, as to whether it is possible to compute statistical averages belonging to infinite random processes using completely deterministic numerical electromagnetic simulation methods. It turns out that this is possible, provided that the physical system satisfies certain conditions. One of the simplest of such situations is when the excitation is *statistically stationary* in time. Stationarity, in its strictest form, means that the statistical properties of the waveforms anywhere in the system *do not* change in time. This is a reasonable assumption for many forms of optical sources and will be made throughout this paper. The study of non-stationary, spectrally partially coherent sources are outside the scope of this review. Interested readers may consult references (Christov, 1986; Lajunen, Vahimaa, & Tervo, 2005; Wang, Lin, Chen, & Zhu, 2003). The importance of stationarity is manifested when the response of a linear system to a stationary time waveform is sought. This is the case in our analysis, because both Maxwell's equations (5)–(8) and the scattering materials are assumed to be linear. Let us consider an input waveform $x_\mathrm{i}(t)$ exciting the system in some way and an output waveform $x_\mathrm{o}(t)$ measured somewhere else. If $x_\mathrm{i}(t)$ is the only excitation, the relation between these is a convolution with the impulse response $h(\tau)$ of the system:

$$x_\mathrm{o}(t) = \int_{-\infty}^{\infty} h(\tau) x_\mathrm{i}(t-\tau)\mathrm{d}\tau. \tag{10}$$

The *transfer function* $H(\omega)$ is defined as the Fourier transform of the impulse response $h(\tau)$,

$$H(\omega) = \int_{\tau=-\infty}^{\infty} h(\tau)\mathrm{e}^{-j\omega\tau}\mathrm{d}\tau. \tag{11}$$

It can be shown that the *power-spectral densities* $S_\mathrm{i}(\omega)$ and $S_\mathrm{o}(\omega)$ of the input and output waveforms are related linearly by the absolute square of the transfer function (Born & Wolf, 1999; Goodman, 2000; Haykin, 2001; Papoulis, 1991):

$$S_\mathrm{o}(\omega) = |H(\omega)|^2 S_\mathrm{i}(\omega). \tag{12}$$

The power-spectral density is an optically relevant and directly measurable quantity, defined as the power at the output of a narrowband filter centered at ω. The Wiener–Khintchine theorem (Born & Wolf, 1999) states that it is also the Fourier transform of the correlation function associated with the stationary waveform. The relation (12) is the central result that connects random waveforms in optics with the deterministic numerical methods of electromagnetics. In a given problem, the power-spectral density of the source $S_\mathrm{i}(\omega)$ is usually known, and the power-spectral density of the output $S_\mathrm{o}(\omega)$ is desired. The necessary link is provided by the absolute square of the transfer function $H(\omega)$. A numerical electromagnetic method can be used to find $H(\omega)$ by sending deterministic signals through the optical system, and calculating the response. Although the majority of the formulas in this review will be given for a fixed frequency ω, the response to a broadband stationary waveform can easily be obtained by repeating the analysis for different ω and using the power-spectral density relation (12).

This repetition becomes unnecessary if a time-domain method is used to obtain the scattering response. In such a case, $H(\omega)$ can be directly obtained at a range of frequencies via temporal Fourier transform of the time-domain response.

3. STRUCTURE OF THE OPTICAL IMAGING SYSTEM

An optical imaging system can be decomposed into several subsystems, each performing a self-contained task that is simple enough to model theoretically. Once the theoretical underpinnings of each subsystem are laid out, the numerical computation of actual physical parameters concerning the subsystem (transmission coefficients, far-field intensities, aberrations, etc.) becomes a matter of approximating the analytical equations in a suitable manner. We represent the optical imaging system as a combination of four subsystems: illumination, scattering, collection, and refocusing. These subsystems are drawn schematically in Figure 1.

3.1 Illumination

The light source and the lens system (usually called the condenser) that focuses the light created by the source onto the object are included in this subsystem. The last lens in the condenser system is shown on the left-hand side of Figure 1, along with the wavefront W_i incident on the object. We will base our review of illumination systems on whether they are *spatially coherent* or *incoherent*. Temporal coherence is a secondary concern since the sources considered in this review are always stationary (see Section 2). Once the responses to all the frequencies in the temporal spectrum of the source

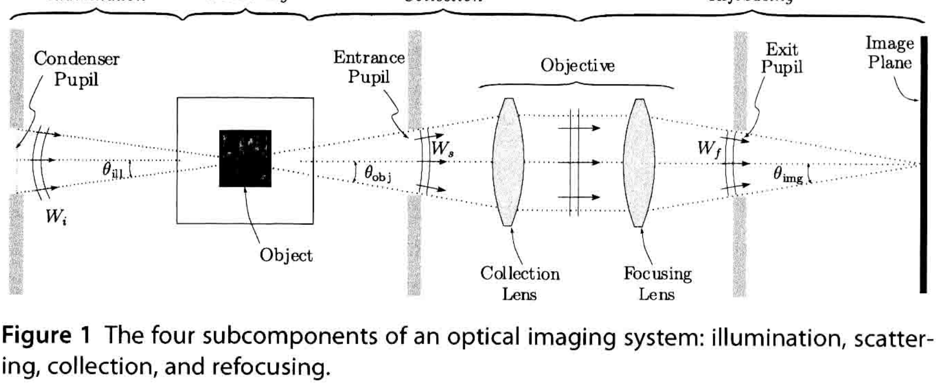

Figure 1 The four subcomponents of an optical imaging system: illumination, scattering, collection, and refocusing.

are found, then the synthesis of the output intensity is simply a matter of adding the intensities of the responses at each frequency.

3.1.1 Coherent Illumination

Spatially coherent illumination means that different points on the illumination beam are fully coherent. This kind of illumination can be created by an infinitesimally small light source, or by an atomic process called stimulated emission, as with lasers. Numerical models with varying degrees of complication are used to represent coherent beams. The simplest coherent illumination method used in numerical modeling is the *plane-wave illumination*. Being invariant in all but one dimension, the plane wave is one of the most basic solutions to Maxwell's equations, wherein the planes of constant phase are all perpendicular to the direction of propagation $\hat{\boldsymbol{k}}_i$. The electric and magnetic field vectors of the plane wave are perpendicular to each other and $\hat{\boldsymbol{k}}_i$. Individually, the plane wave can approximate a more complicated coherent illumination scheme over a very small illumination angle θ_{ill} (Salski & Gwarek, 2009b; Tanev, Tuchin, & Paddon, 2006). Full treatments of some of these illumination schemes in large-θ_{ill} cases have also been considered in the literature, albeit with less popularity. This is primarily because non-planar coherent beams are often difficult to compute and/or implement numerically. One of the more popular coherent illumination beams is the Gaussian beam (Smith, 1997). Although it has an approximate closed-form analytical expression that can be used in limited cases (Salski, Celuch, & Gwarek, 2010; Salski & Gwarek, 2008, 2009a), it is often decomposed into its plane-wave components; resulting in a more accurate description than the more limited closed-form expression (Yeh, Colak, & Barber, 1982). This method has the additional advantage of permitting the use of efficient and readily available plane-wave algorithms, such as the total-field/scattered-field (TF/SF) algorithm in FDTD. Since the Gaussian beam is defined at a single frequency, it is readily adapted to frequency-domain methods (Huttunen & Turunen, 1995; Wei, Wachters, & Urbach, 2007; Wojcik et al., 1991b). However, it can also be used in conjunction with the FDTD method in time-harmonic operation (Choi, Chon, Gu, & Lee, 2007; Judkins, Haggans, & Ziolkowski, 1996; Judkins & Ziolkowski, 1995; Simon & DiMarzio, 2007). The plane-wave spectrum (or the angular spectrum) method can also be used to synthesize arbitrary coherent illumination beams of non-Gaussian shape (Aguilar & Mendez, 1994; Aguilar, Mendez, & Maradudin, 2002). A practical example of a coherent beam is the electromagnetic field distribution around the focal region of an aplanatic lens excited by a plane wave, derived by Richards and Wolf (Richards & Wolf, 1959; Wolf, 1959) using the angular-spectrum method. This beam has been used to simulate the coherent illumination in scanning-type confocal or differential-interference contrast (DIC) microscopes (Munro & Török, 2005; Török, Munro, & Kriezis, 2008). An extension of this technique to time-domain focused pulses was described in (Capoglu, Taflove, & Backman, 2008), which can be used to simulate either ultrafast optical pulses (Davidson & Ziolkowski, 1994; Gu & Sheppard, 1995; Ibragimov, 1995; Kempe, Stamm, Wilhelmi, & Rudolph, 1992; Veetil, Schimmel, Wyrowski, & Vijayan, 2006), or stationary broadband systems via temporal Fourier analysis. The latter type of systems have recently become feasible with the development of white-light laser sources (Booth, Juskaitis, & Wilson, 2008; Coen et al., 2002).

The plane-wave illumination is also sufficient when the scatterer under consideration is very thin compared to the wavelength and/or the range of illumination angles is sufficiently narrow. For example, under the thin-mask assumption (see Section 3.2) in photolithography, scattering from any plane wave from an arbitrary direction is completely determined by the scattering from a plane-wave incident normally on the thin mask. This is because the thin mask is assumed to simply impart a position-dependent phase shift on the plane wave upon transmission. If the scattered wave is decomposed into its angular spectrum (which is continuous if the mask is non-periodic, and discrete if it is periodic), it can easily be shown that this angular spectrum will *rotate* in the same direction that the incident plane wave is rotated. Therefore, it is only necessary in numerical computation to consider a single normally incident plane wave and calculate the "diffracted orders," as the Fourier components of the scattered wave are commonly called in photolithography. In passing, it is worthwhile to note that this "angular-shift invariance" property of the scattered field from a thin mask is a direct result of the Fourier relationship between the scattered field near the mask and the associated angular spectrum of the scattered field. This can easily be seen by comparison to a linear time-invariant (LTI) system, whose effect on its input is a multiplication by a transfer function in the Fourier (or frequency) domain. Similarly, the angular-shift invariance of the scattered field in the Fourier (or angular) domain is a result of the multiplicative action of the mask on the incident field in the spatial domain.

Illumination modeling generally becomes a harder task when the object space is multilayered. The total-field/scattered-field (TF/SF) algorithm in FDTD has been generalized to handle multilayered spaces (Capoglu &

Smith, 2008; Winton, Kosmas, & Rappaport, 2005; Zhang & Seideman, 2010). The plane-wave TF/SF techniques can be used as building blocks for injecting arbitrary coherent beams into a multilayered space, since any beam can in principle be decomposed into a plane-wave spectrum.

3.1.2 Incoherent Illumination

The term "incoherent illumination" is traditionally used to designate an illumination scheme that exhibits partial spatial coherence over the illumination area. Incoherent illumination occurs when the light source has finite spatial extent, with every point on the source radiating in an incoherent fashion. This is an adequate model for many natural and artificial light sources such as the sun, a xenon arc lamp, or a tungsten filament. Incoherence also requires that the excitation source have a finite bandwidth, however small it may be. In fact, the converse of this requirement (strict monochromaticity) is very hard to achieve, for even the most coherent laser sources have a finite bandwidth.

Perhaps the most prominent incoherent illumination scheme in use today is called *Köhler illumination* (Born & Wolf, 1999; Nolte, Pawley, & Höring, 2006, chap. 6), named after August Köhler who designed it in the late 1800s. One of the key advantages of this scheme is that it provides spatially uniform illumination throughout the sample, regardless of the inhomogeneities of the light source. This is accomplished by sending a collimated beam on the sample for every infinitesimal point on the light source. The details of Köhler illumination are shown schematically in Figure 2. The light source on the left of Figure 2 is imaged on the aperture stop by an auxiliary lens. The image of the light source on the aperture stop acts as a secondary source for the succeeding portion of the system. Unlike the original light source, the spatial coherence length on this secondary

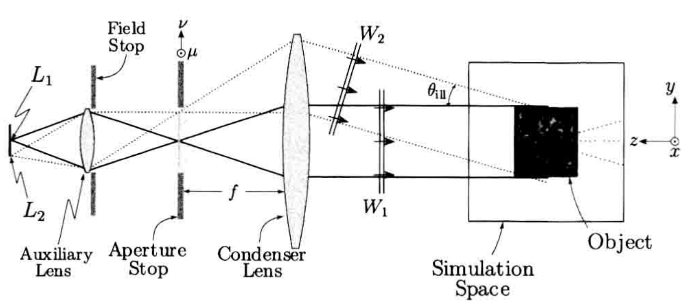

Figure 2 Schematical illustration of Köhler illumination.